Jiang *et al. Chem. Synth.* **2025**, *5*, 6
DOI: 10.20517/cs.2024.36

Chemical Synthesis

Research Article

Open Access

Construction of a novel tetraphenylethylene-based supramolecular dimer for improving the generation of reactive oxygen species and photocatalytic performance

Man Jiang[1,#], Xin-Long Li[2,#], Ning Han[2], Xian-Ya Yao[2], Fa-Dong Wang[2], Kai-Kai Niu[2], Hui Liu[2], Shengsheng Yu[2], Ling-Bao Xing[2,*]

[1]School of Resources and Environmental Engineering, Shandong University of Technology, Zibo 255000, Shandong, China.
[2]School of Chemistry and Chemical Engineering, Shandong University of Technology, Zibo 255000, Shandong, China.
[#]Authors contributed equally.

[*]**Correspondence to:** Prof. Ling-Bao Xing, School of Chemistry and Chemical Engineering, Shandong University of Technology, 266 Xincun West Road, Zhangdian District, Zibo 255000, Shandong, China. E-mail: lbxing@sdut.edu.cn

How to cite this article: Jiang, M.; Li, X. L.; Han, N.; Yao, X. Y.; Wang, F. D.; Niu, K. K.; Liu, H.; Yu, S.; Xing, L. B. Construction of a novel tetraphenylethylene-based supramolecular dimer for improving the generation of reactive oxygen species and photocatalytic performance. *Chem. Synth.* **2025**, *5*, 6. https://dx.doi.org/10.20517/cs.2024.36

Received: 20 Mar 2024 **First Decision:** 4 Jun 2024 **Revised:** 4 Jul 2024 **Accepted:** 5 Jul 2024 **Published:** 10 Aug 2024

Academic Editor: Jin Xie **Copy Editor:** Pei-Yun Wang **Production Editor:** Pei-Yun Wang

Abstract

Using supramolecular strategies to improve the generation of reactive oxygen species is a practical and environmentally friendly method, but it is also a difficult undertaking. In this study, we created and produced a vinylpyridine-modified tetraphenylethylene derivative TPE-Py-I, which has excellent solubility in water and has the ability to construct supramolecular dimers (2TPE-Py-I@CB[8]) in an aqueous solution through host-guest interaction with cucurbit[8]uril (CB[8]). The supramolecular dimer demonstrated a remarkable aggregation-induced emission response, with the fluorescence progressively intensifying upon the introduction of CB[8]. Meanwhile, the formation of supramolecular dimer also greatly improved the intersystem crossing effect of the molecular assembly system, so that the generation ability of reactive oxygen species including singlet oxygen ($^1O_2$) and superoxide anion radical ($O_2^{\bullet-}$) were enhanced, which provided a basis for its application as an excellent supramolecular photosensitizer in photocatalytic organic reactions. To our delight, 2TPE-Py-I@CB[8] exhibits excellent photocatalytic properties, making it suitable for both phosphine photooxidation and cross-dehydrogenative coupling reactions. This work provides a non-covalent strategy for the development of supramolecular dimer photosensitizers and broadens its application in the field of photocatalytic organic conversion.

Keywords: Supramolecular dimer, reactive oxygen species, photocatalyst, photooxidation reaction

© The Author(s) 2024. **Open Access** This article is licensed under a Creative Commons Attribution 4.0 International License (https://creativecommons.org/licenses/by/4.0/), which permits unrestricted use, sharing, adaptation, distribution and reproduction in any medium or format, for any purpose, even commercially, as long as you give appropriate credit to the original author(s) and the source, provide a link to the Creative Commons license, and indicate if changes were made.

INTRODUCTION

Chemistry, as a foundational field of study, not only produces a diverse range of products for mankind, but also consistently contaminates the environment. Solar energy aligns well with modern chemistry, which emphasizes environmental sustainability, green practices, and efficient use of resources. Organic photochemistry has experienced tremendous development in recent years due to the ongoing research efforts, making it an essential component of modern chemistry. Visible-light-driven photocatalytic organic conversion is a novel area of study in organic photochemistry. It is being intensively researched because of its benefits, including environmental friendliness, gentle reaction conditions, and high catalytic efficiency[1-4]. A photosensitizer or photocatalyst is crucial in facilitating photocatalytic organic conversion. Under specific wavelengths of light, they can typically be stimulated to form excited state intermediates, and the energy of the intermediates can be released to substrates, through energy transfer (EnT) or electron transfer (ET). This process generates various reactive oxygen species (ROS) and active intermediates that can achieve catalytic effects[5-7]. According to the production mechanism, photooxidation can be divided into two categories: ET and EnT processes. The ET process, which was type I process, involves the conversion of a ground state molecule into an excited state photosensitive molecule through targeted light exposure and then undergoes ET with the substrate molecule and formed a variety of free radical intermediates. Subsequently, oxygen, water, *etc.*, extinguish the sensitizer anion free radical and generate superoxide anion free radical ($O_2^{\bullet-}$)[8,9]. The EnT process is referred to as the type II process where the excited photosensitive molecules transfer energy directly to oxygen, water, and other substances, and then return to their original form. This transfer of energy also leads to the generation of singlet oxygen ($^1O_2$)[10]. Consequently, an exceptional photosensitizer or photocatalyst should be equipped with the following benefits: (1) good light stability and excellent long-lived triplets[11-14]; (2) the ability to facilitate efficient EnT or ET.

Photosensitizers and photocatalysts can be categorized into two groups: metal-[15,16] and non-metal-based[17,18]. Despite their benefits in terms of excellent light stability and high catalytic efficiency, both options are still costly, have limited availability in natural reserves, and require complex adaptations, among other drawbacks. Simultaneously, conventional photosensitizers exhibit both low fluorescence intensity and limited applicability due to the aggregation-caused quenching (ACQ) phenomenon[19-21], which hinders their ability to efficiently generate ROS. Hence, the development of water-based ROS production devices that may circumvent these drawbacks continues to be a formidable undertaking. Thankfully, the issue has been effectively resolved by the development of photosensitizers that exhibit aggregation-induced emission (AIE) properties[22-25]. Furthermore, the prohibition of non-radiative transitions allows AIE-based photosensitizers to generate an adequate amount of ROS while in an aggregated form[26,27]. For example, in 2020, Qian *et al.* developed a smart system for generating $^1O_2$ using AIE molecules. The creation of $^1O_2$ can be controlled by adjusting the molar ratio between the macrocyclic host and the guest molecule[28]. Zuo *et al.* reported a supramolecular system. It can efficiently produce $^1O_2$ and participate in the conversion process of dopamine to polydopamine as a photocatalyst[29]. Nevertheless, the task of developing AIE photosensitizers using supramolecular methods to enhance their capacity for generating ROS and improving their efficiency in photocatalytic organic conversion remains a formidable problem.

Tetraphenylethylene (TPE) and its derivatives, as classic AIE groups, not only have excellent fluorescence properties, but also have good ROS production capacity. They have been widely used in fluorescence imaging, ion detection, artificial light-harvesting systems, photodynamic therapy, *etc.*[30-39]. Nevertheless, the utilization of this approach in the fabrication of supramolecular dimers for the purpose of photosensitization and photocatalysis has received limited attention. In this work, we designed and

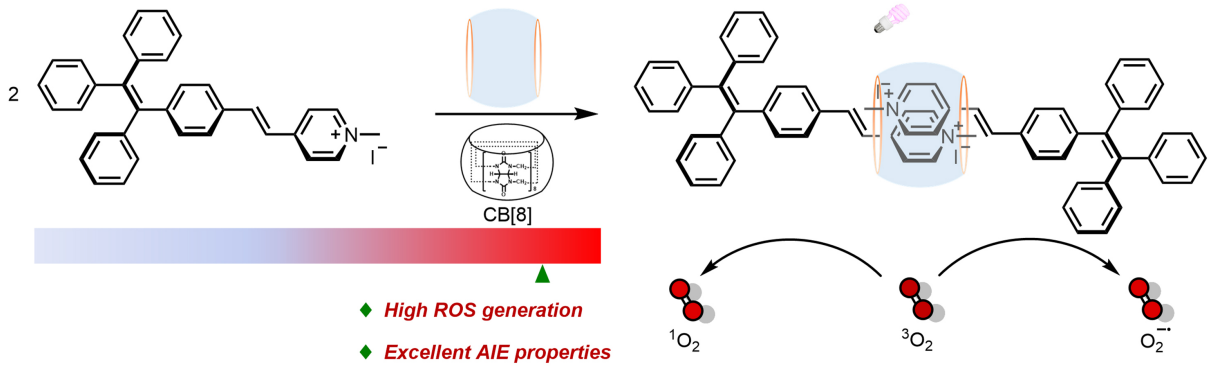

Scheme 1. Schematic diagram of 2TPE-Py-I@CB[8] and the photocatalytic ROS generation. ROS: Reactive oxygen species.

synthesized a vinylpyridine-modified TPE derivative (TPE-Py-I), which had good water solubility and can form a supramolecular dimer (2TPE-Py-I@CB[8]) with CB[8] [Scheme 1]. The formation of 2TPE-Py-I@CB[8] not only enhanced fluorescence properties, but also greatly promoted the generation of ROS, making 2TPE-Py-I@CB[8] a better photosensitizer, which can be further used as an efficient photocatalyst for photooxidation of phosphine and cross-dehydrogenative coupling (CDC) reactions with the yields up to 90% and 85%. This study presents an approach for developing photocatalysts using supramolecular dimers, which expands their potential for use in photocatalytic organic conversion[40,41].

EXPERIMENTAL

Materials

Unless specifically mentioned, the chemicals used are commercially available. The compound TPE-Py-I was obtained by a two-step reaction using 1-(4-bromophenyl)-1,2,2-triphenylethylene (98%, Shanghai Bide Medical Technology Co., LTD), 4-vinylpyridine (99%, Shanghai Titan Technology Co., LTD), and iodomethane (99%, Shanghai Titan Technology Co., LTD) as raw materials. Pd(PPh3)2Cl2 [98% (AR)], triphenylphosphine [99% (AR)], potassium carbonate [99% (AR)], anhydrous sodium sulfate [99% (AR)], tetrahydroisoquinoline [99% (AR)], and iodobenzene [99% (AR)] were purchased from Shanghai Titan Technology Co., LTD.

Characterizations

Hydrogen nuclear magnetic resonance (^{1}H NMR) and carbon nuclear magnetic resonance (^{13}C NMR) were characterized on Bruker Avance 400 NMR instrument. Ultraviolet-visible (UV-vis) absorption spectra were characterized by a Shimadzu UV-2450 spectrophotometer. Fluorescence emission spectra were obtained by fluorescence spectrophotometer F-380A. Dynamic light scattering (DLS) and Zeta potential tests were constructed on Malvern Zeta sizer Nano ZS90. The photocatalytic reaction was performed on WATTCAS Parallel Photocatalytic Reactor (WP-TEC-HSL) with 10W COB LED. Electron Paramagnetic Resonance (EPR) was characterized on Bruker EMXplus-6/1.

Synthesis of TPE-Py-I

The target molecule TPE-Py-I[42-44] was synthesized [Supplementary Scheme 1]. Compound A (217 mg, 0.5 mmol) and iodomethane (710 mg, 5.0 mmol) were dissolved in 5.0 mL N,N-dimethylformamide (DMF) and reacted for 12 h at 100 °C. The reaction mixture was then cooled to room temperature, and acetone was added to precipitate the solid. The precipitate was washed using acetone to obtain an orange solid (173 mg, 0.30 mmol) with a yield of 60%. ^{1}H NMR (400 MHz, DMSO-d_6) δ 8.84 (d, J = 6.5 Hz, 2H), 8.20-8.14 (m, 2H), 7.90 (d, J = 16.3 Hz, 1H), 7.52 (d, J = 8.3 Hz, 2H), 7.43 (d, J = 16.3 Hz, 1H), 7.20-7.12 (m, 9H), 7.08-7.05 (m,

2H), 7.00 (m, 6H), 4.24 (s, 3H). ^{13}C NMR (101 MHz, DMSO-d_6) δ 152.84, 145.94, 145.54, 143.44, 143.37, 143.20, 142.03, 140.55, 140.38, 133.76, 131.90, 131.19, 131.17, 131.09, 128.45, 128.33, 128.13, 127.34, 127.27, 127.22, 123.89, 123.63, 47.39. HRMS: [electrospray ionisation (ESI)] m/z calcd for $C_{34}H_{28}N$ [M-I]$^+$: 450.2216, found: 450.2209.

RESULTS AND DISCUSSION

TPE-Py-I was an orange solid and characterized by ^{1}H NMR, ^{13}C NMR and infrared spectroscopy (IR) [Supplementary Figures 1-4], which has good solubility and provides an excellent basis for TPE-Py-I to construct supramolecular dimers in the aqueous solution. To explore the host-guest interaction between TPE-Py-I and CB[8], UV-Vis absorption spectra and fluorescence emission spectra were employed for characterization. It can be observed from Figure 1A and B that TPE-Py-I had maximum absorption and maximum emission peaks at 384 and 580 nm, respectively. Figure 1A showed that the addition of CB[8] made the TPE-Py-I experience a slight decrease and redshift. This indicated that CB[8] successfully encapsulated the pyridine group. In addition, the absorption spectra no longer changed after adding 0.5 equiv. CB[8]. It showed that the combination of TPE-Py-I and CB[8] was balanced and the binding ratio of TPE-Py-I and CB[8] was 2:1. The change of fluorescence emission spectra also reflects the combination process of TPE-Py-I and CB[8]. The emission peak increased significantly and redshifted from 580 to 600 nm after gradually adding CB[8], and the fluorescence color changed from yellow to orange. Interestingly, the fluorescence emission peak no longer increased after adding 0.5 equiv. CB[8] [Figure 1B], which further confirms the binding ratio of TPE-Py-I and CB[8] was 2:1.

In addition, the Job's plot was used to explore the binding stoichiometric ratios of TPE-Py-I and CB[8] [Figure 1C]. The total concentration of TPE-Py-I and CB[8] was set at a fixed value of 10 μM. The binding ratio was obtained by measuring the fluorescence intensity of TPE-Py-I/TPE-Py-I + CB[8] aqueous solutions with varying molar ratios. During this procedure, it was observed that the fluorescence intensity reached its highest level at a TPE-Py-I/TPE-Py-I + CB[8] ratio of 0.66, which suggests that the binding ratio of TPE-Py-I and CB[8] in the aqueous solution was 2:1. Subsequently, we further investigated the interaction between TPE-Py-I and CB[8] by using ^{1}H NMR spectroscopy experiments. As can be seen from Supplementary Figure 5, CB[8] has a low field displacement [Supplementary Table 1] with the addition of CB[8], and H_a on the methyl group of TPE-Py-I has a shift to the high field region [Supplementary Table 1]. The proton signal of H_b and H_c was decreased, but no chemical shift was generated. Moreover, the ^{1}H NMR pattern does not change at all when adding more CB[8], which further proves that the combination ratio of TPE-Py-I and CB[8] was 2:1.

DLS and zeta potential were employed to characterize the self-assembly behavior of TPE-Py-I and CB[8] for further study. Figure 1D demonstrates that the particle size of 2TPE-Py-I@CB[8] was around 500 nm, exhibiting a prominent Tyndall effect. This observation supports the presence of substantial aggregates of 2TPE-Py-I@CB[8]. Furthermore, the alteration of zeta potential can provide evidence for the interaction between TPE-Py-I and CB[8]. The potential of TPE-Py-I in the aqueous solution was determined to be +32.5 mV [Figure 1E and F]. Interestingly, after the formation of 2TPE-Py-I@CB[8], the potential experienced a reduction to +15.1 mV. The presence of the hydrophobic cavity of CB[8] surrounding TPE-Py-I may have resulted in an electrostatic shielding effect and a decrease in potential.

As the fluorescent chromophore of supramolecular dimer 2TPE-Py-I@CB[8], TPE not only exhibited excellent optical properties to avoid the ACQ effect, but also has excellent ROS generation ability. Therefore, 2,7-dichlorodihydrofluorescein diacetate (DCFH-DA) was first used as a fluorescent probe for ROS generation and monitored by fluorescence emission spectroscopy to explore the ability of TPE-Py-I to

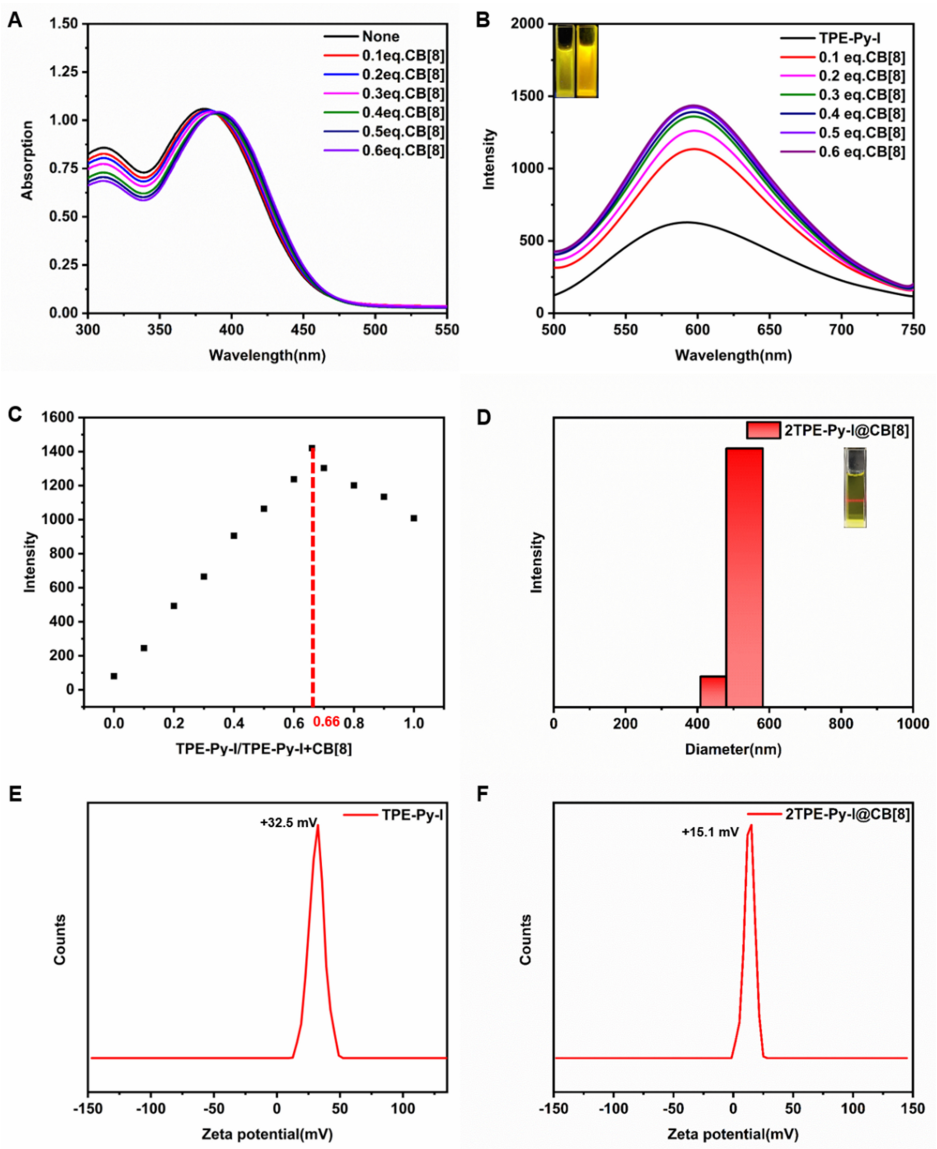

Figure 1. (A) UV-vis absorption spectra of TPE-Py-I with the gradual addition of CB[8]; (B) Fluorescence emission spectra (λ_{ex} = 384 nm) of TPE-Py-I with the gradual addition of CB[8]; the inset was the fluorescence images of TPE-Py-I (left) and 2TPE-Py-I@CB[8] (right); (C) Job's plot of TPE-Py-I and CB[8]; (D) DLS of 2TPE-Py-I@CB[8], the inset was Tyndall effect of 2TPE-Py-I@CB[8]; Zeta potential of (E) TPE-Py-I and (F) 2TPE-Py-I@CB[8]. (Experimental conditions: TPE-Py-I = 10 μM, CB[8] = 5 μM, room temperature.) UV-vis: Ultraviolet-visible; TPE: tetraphenylethylene; DLS: dynamic light scattering.

produce ROS before and after addition of CB[8] [Supplementary Materials]. As shown in Supplementary Figures 6 and 7, a new fluorescence emission peak appeared at 525 nm but without any change when only DCFH-DA was added to the aqueous solution and irradiated by purple light for different times. Subsequently, the same concentration of DCFH-DA was added to the aqueous solution of TPE-Py-I and irradiated for the different times, and the emission peak at 525 nm was continuously enhanced with the increase of irradiation time. Similarly, the emission peak of 2TPE-Py-I@CB[8] aqueous solution at 525 nm also increased continuously with the increase of irradiation time, and the increase is even more pronounced compared to TPE-Py-I. This indicated that supramolecular dimerization significantly enhanced the ROS production capacity. Subsequently, the production of singlet oxygen ($^1O_2$) was detected by UV-Vis absorption spectrum and 9,10-anthracenediyl-bis(methylene)-dimalonic acid (ABDA) as $^1O_2$ probe

[Supplementary Materials]. The ability of $^1O_2$ generation can be well compared according to the decrease of the absorption peak of ABDA at 378 nm. As shown in Figure 2A and Supplementary Figure 8, the ABDA containing 2TPE-Py-I@CB[8] decreased most significantly after the same time of exposure to purple light. These results suggest that 2TPE-Py-I@CB[8] has a better ability to produce $^1O_2$. Furthermore, in order to quantitatively detect the $^1O_2$ production capacity of TPE-Py-I and 2TPE-Py-I@CB[8], we chose Rose Bengal (RB) as the reference photosensitizer to explore. The singlet oxygen efficiency of RB (Φ_{RB}) in aqueous solution was 0.75. Subsequently, according to the calculation method in Supplementary Figure 9, the singlet oxygen efficiency of 2TPE-Py-I@CB[8] was 1.29, and the singlet oxygen efficiency of TPE-Py-I was 0.57. In addition, N,N,N',N'-tetramethyl-phenylenediamine (TMPD) was selected as the trapping agent of $O_2^{\bullet-}$, and its production was monitored by UV-vis absorption spectroscopy [Supplementary Materials]. As shown in Figure 2B, when only TMPD was added to the aqueous solution, the absorption of TMPD barely changed after being irradiated under purple light for 1 min. However, when the same concentration of TMPD was added to the TPE-Py-I aqueous solution and irradiated with the same light for 1min, two new absorption peaks appeared at 563 and 612 nm. Excitingly, the 2TPE-Py-I@CB[8] aqueous solution increased most obviously under the same condition. The above results show that the formation of supramolecular dimer 2TPE-Py-I@CB[8] significantly improves the intersystem crossing (ISC) efficiency, thus improving the efficiency of EnT and ET, and making 2TPE-Py-I@CB[8] a more excellent photosensitizer.

To further confirm the production of active species, EPR studies were conducted. The compound 2,2,6,6-tetramethylpiperidine (TEMP) was chosen as a means to capture $^1O_2$, while 5,5-dimethyl-1-pyrrolin-N-oxide (DMPO) was employed as a probe to detect $O_2^{\bullet-}$. Figure 2C demonstrates that the introduction of TEMP to a water-based solution of 2TPE-Py-I@CB[8] did not result in any detectable signal under low light conditions. Following a period of 1 min of exposure to purple light, a distinct signal became visible. In the absence of light, the introduction of DMPO to a water-based solution containing 2TPE-Py-I@CB[8] did not generate any detectable response. Following 1 min exposure to purple light, a distinct signal became visible [Figure 2D]. The results demonstrate that 2TPE-Py-I@CB[8] has the ability to generate both $^1O_2$ and $O_2^{\bullet-}$ concurrently.

ROS can be used as photoactive substances and play a crucial role in photoredox reactions. Since 2TPE-Py-I@CB[8] can produce ROS, it can be used as photocatalysts for photocatalytic organic conversion. Initially, triphenylphosphine was chosen as the template substrate and subjected to the photooxidation reaction under various circumstances. Table 1 demonstrates that under ideal circumstances, 2TPE-Py-I@CB[8] exhibited remarkable catalytic ability, resulting in a triphenylphosphine oxide yield of 90% (entry 1). Nevertheless, TPE-Py-I exhibited limited catalytic efficiency under the same circumstances, resulting in only a 17% yield (entry 2). Simultaneously, the quantity of catalyst had a significant influence on the oxidation efficiency, resulting in a substantial decrease in yield to 61% when the catalyst quantity was reduced to 0.5 mol% (entry 3). Enhancing the catalyst amount to 1.5 mol% yields negligible impact on the outcome of this reaction (89%, entry 4). Furthermore, decreasing the time of irradiation to 12 h significantly decreased the yield to 56% (entry 5), but increasing the time of irradiation resulted in minimal change in the yield (92%, entry 6). The controlled studies demonstrated that the production of triphenylphosphine oxide in aqueous solution was nearly nonexistent without the presence of purple light irradiation (entry 7) and photocatalyst (entry 8), highlighting the essential role of light and photocatalyst in the reaction. In addition, we also explored the reaction temperature and found that the yield of the reaction was reduced (entry 9) by lowering the temperature to 10 °C, while the yield of the reaction was slightly increased by raising the temperature to 40 °C (entry 10), indicating that room temperature is the optimal reaction condition.

Table 1. 2TPE-Py-I@CB[8] as photocatalysts for photooxidation of phosphine under different conditions

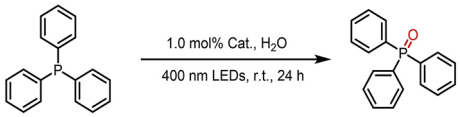

Entry	Deviation from standard conditions	Yield[b] (%)
1	None[a]	90
2	1.0 mol% TPE-Py-I instead of 1.0 mol% 2TPE-Py-I@CB[8]	17
3	0.5 mol% 2TPE-Py-I@CB[8] instead of 1.0 mol% 2TPE-Py-I@CB[8]	61
4	1.5 mol% 2TPE-Py-I@CB[8] instead of 1.0 mol% 2TPE-Py-I@CB[8]	89
5	12 h instead of 24 h	56
6	48 h instead of 24 h	92
7	Without light	NR
8	Without 2TPE-Py-I@CB[8]	NR
9	10 °C instead of RT	73
10	40 °C instead of RT	93

[a]Reaction conditions: triphenylphosphine (0.2 mmol, 52 mg), purple light (400 nm), 2TPE-Py-I@CB[8] aqueous solution (1.0 mol%, 2.0 mL), room temperature, 24 h; [b]Isolated yield. TPE: Tetraphenylethylene; NR: no reaction; RT: room temperature.

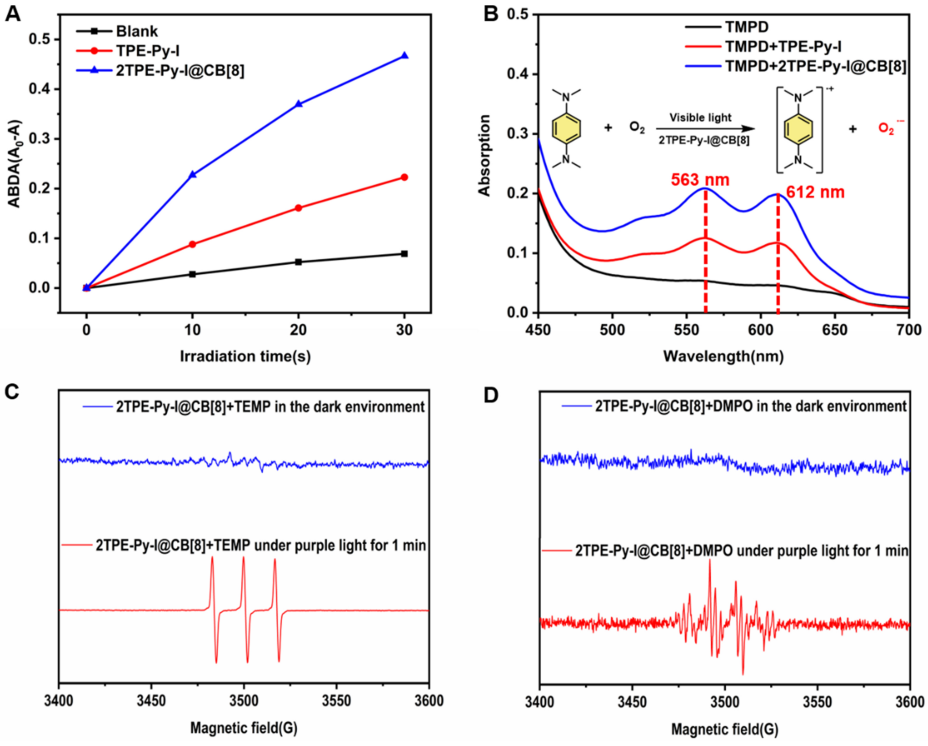

Figure 2. (A) Plots of A_0-A for ABDA at 378 nm upon purple light (400 nm, 10 W) irradiated for different times in the presence of ABDA, TPE-Py-I + ABDA or 2TPE-Py-I@CB[8] + ABDA; (B) the UV-vis absorption spectra of TMPD at 563 and 612 nm upon purple light (400 nm, 10 W) irradiation for 1 min in the presence of TMPD, TPE-Py-I + TMPD or 2TPE-Py-I@CB[8] + TMPD; (C) 2TPE-Py-I@CB[8] with TEMP placed in the dark environment or irradiated with purple light (400 nm, 10 W) for 1 min; (D) 2TPE-Py-I@CB[8] with DMPO placed in the dark environment or irradiated with purple light (400 nm, 10 W) for 1 min. (Experimental condition: TPE-Py-I = 20 μM, CB[8] = 10 μM, ABDA = 50 μM, TMPD = 100 μM, TEMP = 200 μM, DMPO = 200 μM.) ABDA: 9,10-anthracenediyl-bis(methylene)-dimalonic acid; TPE: tetraphenylethylene; UV-vis: ultraviolet-visible; TMPD: N,N,N′,N′-tetramethyl-phenylenediamine; TEMP: 2,2,6,6-tetramethylpiperidine; DMPO: 5,5-dimethyl-1-pyrrolin-N-oxide.

After determining the optimal reaction conditions, different phosphine derivatives were selected to investigate the universality and stability of 2TPE-Py-I@CB[8] on the photooxidation reactions of phosphine. It can be seen from Figure 3 that 2TPE-Py-I@CB[8] showed excellent ability for all substrates (electron-withdrawing and electron-donating groups [Supplementary Figures 10-39]). The yields of substrates **2b**, **2c** and **2d** were 89%, 92% and 82%, respectively. In addition, 2TPE-Py-I@CB[8] still had a good catalytic effect when the substituents were located in the meta-position of triphenylphosphine. The results showed that the yields of **2e**, **2f**, and **2g** were 84%, 75%, and 72%, respectively. In particular, when the substituent was pyridine, 2TPE-Py-I@CB[8] also showed good catalytic capacity with a yield of 91% (**2h**). Similarly, the yields reached 88% (**2i**) and 81% (**2j**) when the substituents were located in the ortho-position of triphenylphosphine. In addition, when substituents were propyl, methyl and cyclohexane, 2TPE-Py-I@CB[8] had better catalytic effect with yields of 87% (**2k**) , 94% (**2l**) and 83% (**2m**), respectively. Surprisingly, 2TPE-Py-I@CB[8] had an excellent catalytic effect on tricyclohexylphosphine with a yield of up to 79% (**2n**). For phosphine derivatives with two oxidation sites, 2TPE-Py-I@CB[8] still had a good oxidation effect with a yield of up to 80% (**2o**). The results show that 2TPE-Py-I@CB[8] has a good ability to catalyze the photooxidation of phosphines.

In addition, we also found that 2TPE-Py-I@CB[8] can be used as an excellent photocatalyst for CDC reaction. As shown in Table 2, N-phenyltetrahydroisoquinoline and indole served as substrates to screen different conditions. Under optimal circumstances, 2TPE-Py-I@CB[8] exhibited exceptional catalytic ability, yielding up to 85% (Supplementary Figure 40, entry 1). Nevertheless, TPE-Py-I exhibited a low catalytic efficiency under the same circumstances, resulting in only a 21% yield (entry 2). Simultaneously, the quantity of catalyst had a significant influence on the CDC reaction, resulting in a substantial decrease in yield to 51% when the catalyst amount was decreased to 0.5 mol% (entry 3). By increasing the catalyst amount to 1.5 mol%, the yield experienced a marginal improvement to 87% (entry 4). Furthermore, decreasing the time of irradiation to 12 h caused a lower yield to 61% (entry 5), but increasing the time of irradiation to 48 h had minimal impact on the yield (86%, entry 6). The controlled studies demonstrated that the absence of purple light irradiation (entry 7) and photocatalyst (entry 8) resulted in no product formation in the aqueous solution. This suggests that both light and photocatalyst are crucial factors in the reaction. In addition, we also explored the reaction temperature and found that the yield of the reaction was reduced (entry 9) by lowering the temperature to 10 °C, while the yield of the reaction was slightly increased by increasing the temperature to 40 °C (entry 10), indicating that room temperature is the optimal reaction condition.

After determining the optimal reaction conditions, different N-phenyltetrahydroisoquinoline derivatives and indole derivatives were reacted to explore the universality and stability of 2TPE-Py-I@CB[8] [Supplementary Figures 40-57]. Initially, various N-phenyltetrahydroisoquinoline derivatives were used to react with indole. It can be seen from Figure 4 that 2TPE-Py-I@CB[8] showed remarkable catalytic efficiency for substrates containing both electron-withdrawing and electron-donating groups. The yields of substrates **4b**, **4c**, **4d** and **4e** were 83%, 84%, 82% and 71%, respectively. Notably, the yield decreased when different indole derivatives reacted with N-phenyltetrahydroisoquinoline. The yields of substrates **4f**, **4g**, **4h** and **4i** were 78%, 76%, 70% and 68%, respectively. Our results show that 2TPE-Py-I@CB[8] shows remarkable stability and universality when used as a photocatalyst for CDC reactions.

In addition, to explore the main active species involved in the photooxidation of phosphine and CDC reactions, triethylamine (TEA), potassium iodide (KI), sodium azide (NaN_3) and DMPO were used as scavengers of hydroxyl radical ($^{\bullet}OH$) and hole (h^+), $^1O_2$ and $O_2^{\bullet-}$[45,46]. First, the photooxidation of phosphine was performed under optimal conditions. As shown in Figure 5A, the yields basically did not change with

Table 2. Yield of CDC reaction of N-phenyltetrahydroisoquinoline and indole under different conditions

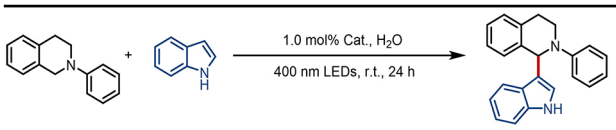

Entry	Deviation from standard conditions	Yield[b] (%)
1	None[a]	85
2	1.0 mol% TPE-Py-I instead of 1.0 mol% 2TPE-Py-I@CB[8]	21
3	0.5 mol% 2TPE-Py-I@CB[8] instead of 1.0 mol% 2TPE-Py-I@CB[8]	51
4	1.5 mol% 2TPE-Py-I@CB[8] instead of 1.0 mol% 2TPE-Py-I@CB[8]	87
5	12 h instead of 24 h	61
6	48 h instead of 24 h	86
7	Without light	NR
8	Without 2TPE-Py-I@CB[8]	NR
9	10 °C instead of RT	76
10	40 °C instead of RT	88

[a]Reaction conditions: N-phenyltetrahydroisoquinoline (20 mg, 0.1 mmol), indole (23.4 mg, 0.2 mmol), 2TPE-Py-I@CB[8] (1.0 mol%, 2.0 mL), purple light (400 nm), room temperature, 24 h; [b]Isolated yields. CDC: Cross-dehydrogenative coupling; TPE: tetraphenylethylene; NR: ; RT: room temperature.

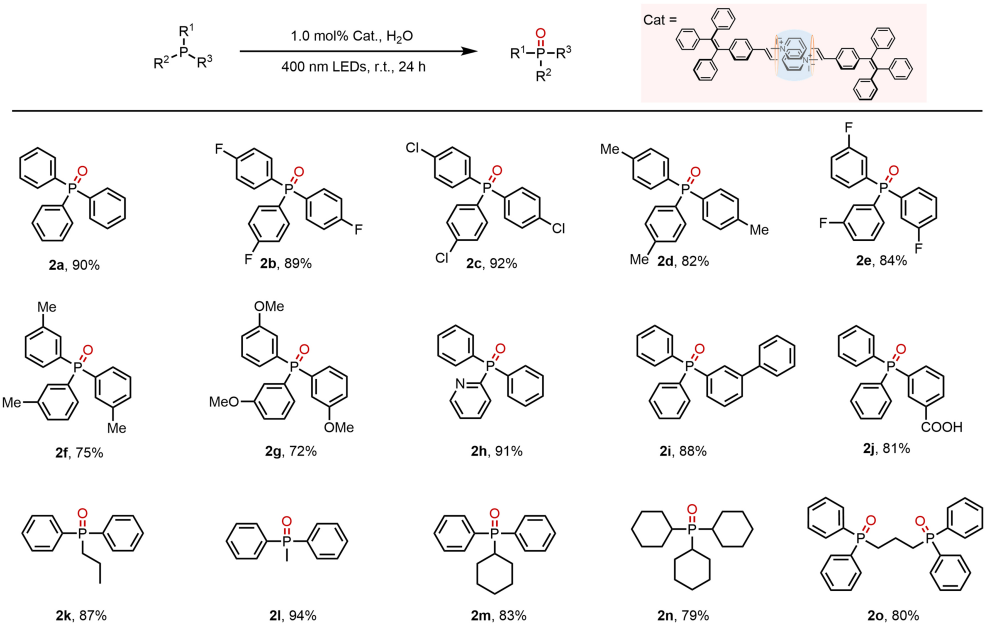

Figure 3. 2TPE-Py-I@CB[8] as photocatalysts to catalyze different phosphine derivatives. Reaction conditions: Phosphine derivatives (0.2 mmol), 2TPE-Py-I@CB[8] aqueous solution (1.0 mol%, 2.0 mL), purple light (400 nm), room temperature, 24 h. Isolated yield. TPE: Tetraphenylethylene.

89% and 88% under purple light for 24 h after adding 0.2 mmol TEA and 0.2 mmol KI. On the contrary, when 0.2 mmol NaN_3 was added and the reaction was carried out under the same conditions, the yield was only 43%. When 0.2 mmol DMPO was added and the reaction was carried out under the same conditions, the yield was slightly reduced to 85%. These results fully indicate that $^1O_2$ is the main active species involved in the photooxidation of phosphine. Similarly, TEA, KI, NaN_3 and DMPO were used as scavengers to participate in CDC reactions.

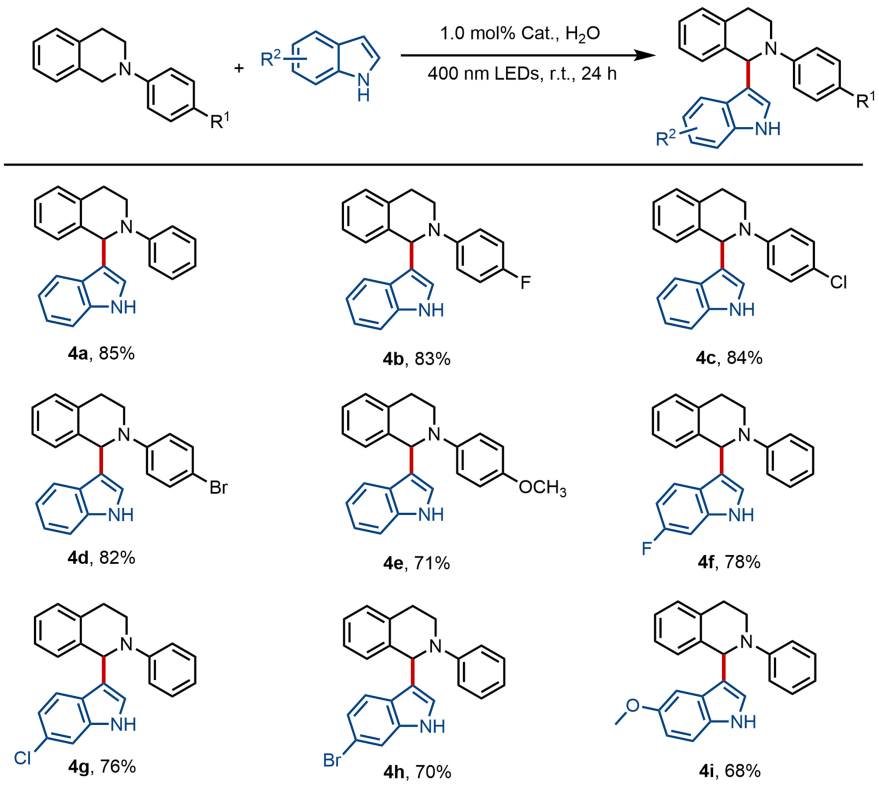

Figure 4. Substrates for CDC reaction. Reaction conditions: N-phenyltetrahydroisoquinoline derivative (0.1 mmol, 1 equiv.), indole derivative (0.2 mmol, 2 equiv.), 2TPE-Py-I@CB[8] (1.0 mol%, 2.0 mL). purple light (400 nm), room temperature, 24 h. Isolated yield. CDC: Cross-dehydrogenative coupling; TPE: tetraphenylethylene.

As shown in Figure 5B, the yield basically did not change after adding 0.2 mmol TEA, 0.2 mmol KI and 0.2 mmol NaN_3 and irradiated under purple light for 24 h with yields of 84%, 82% and 80%, respectively. On the contrary, when 0.2 mmol DMPO was added and the reaction was carried out under the same conditions, the yield was reduced to 20%. These results fully indicate that $O_2^{\bullet-}$ is the main active species involved in CDC reaction. Based on experimental analysis and previous reports[47-49], a possible mechanism of 2TPE-Py-I@CB[8] catalyzed photooxidation of triphenylphosphine and CDC reactions was proposed [Figure 5C]. Firstly, TPE-Py-I@CB[8] was excited by light to reach the excited state {(2TPE-Py-I@CB[8])*}. Subsequently, the excited photocatalyst experiences two pathways. The first pathway involves EnT with $^3O_2$, resulting in $^1O_2$ and ground state photocatalyst. Subsequently, triphenylphosphine reacted with $^1O_2$ and formed intermediate **I** and the $O_2^{\bullet-}$, which then reacted with **I** to produce the product triphenylphosphine oxides. Another pathway was ET with N-phenyltetrahydroisoquinoline to form intermediate **II** and (2TPE-Py-I@CB[8])$^{\bullet-}$. Simultaneously, the hydrogen atom transfer occurs between $O_2^{\bullet-}$ and **II**, resulting in the formation of the nitrogen cations intermediate **III**, which subsequently underwent nucleophilic substitution by indole to provide the desired product.

CONCLUSION

In conclusion, we designed and synthesized a photosensitizer molecule TPE-Py-I with TPE as the skeleton, which had good water solubility and could form supramolecular dimers (2TPE-Py-I@CB[8]) in the aqueous solution through host-guest interactions with CB[8]. Furthermore, the creation of the supramolecular dimer 2TPE-Py-I@CB[8] not only improves the optical characteristics, but also enhances the ability to produce ROS, thereby making 2TPE-Py-I@CB[8] an outstanding water-soluble supramolecular photosensitizer. In

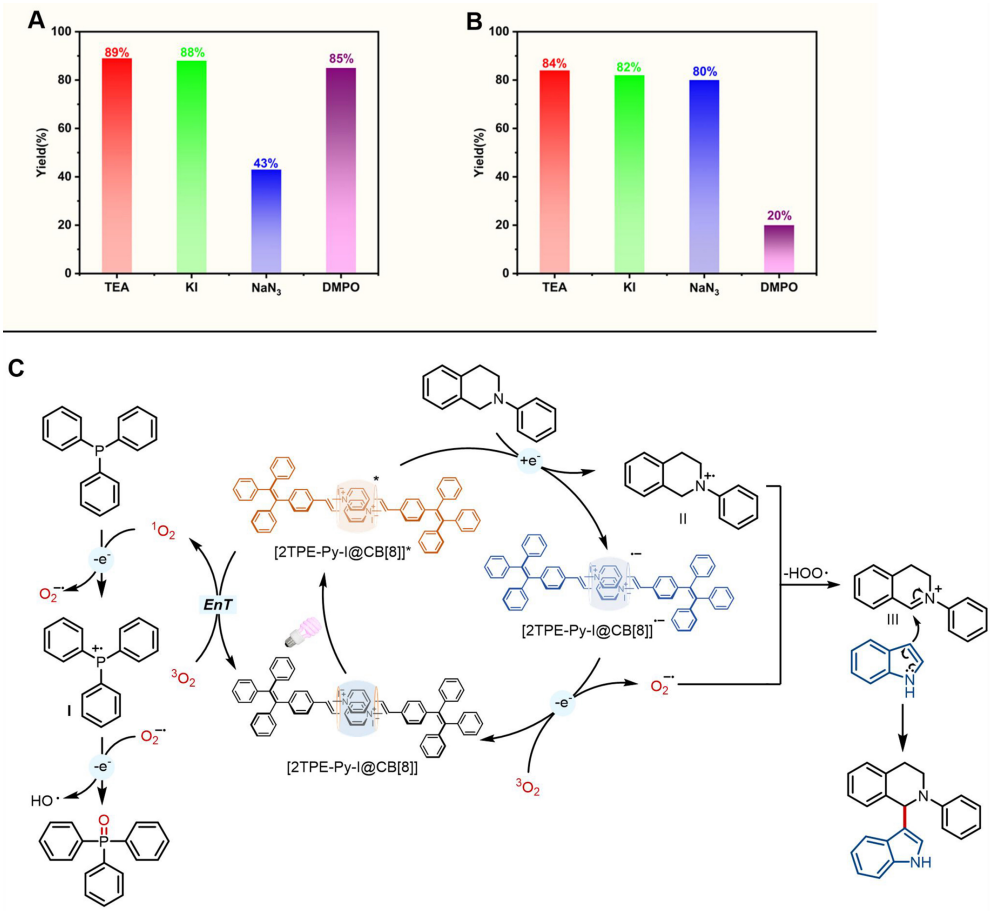

Figure 5. (A) The yields of the photooxidation of phosphine with different scavengers; (B) The yields of CDC reaction with different scavengers; (C) Possible mechanism of photooxidation of phosphine and CDC reactions. CDC: Cross-dehydrogenative coupling.

addition, the system has been effectively utilized in the photooxidation reaction of phosphine and CDC reaction, demonstrating excellent universality and stability. This study expands the potential use of supramolecular photosensitizers in the area of photocatalytic organic conversion.

DECLARATIONS

Authors' contributions

Conception and design of the study: Xing LB
Data collection and analysis: Jiang M, Li XL
Sample preparation: Yao XY, Wang FD, Liu H, Yu S
Paper writing and reviewing: Jiang M, Li XL, Han N, Niu KK, Xing LB

Availability of data and materials

The authors confirm that the detailed experimental and data supporting the findings of this study are available within its Supplementary Materials.

Financial support and sponsorship

We are grateful for the financial support from the National Natural Science Foundation of China (52205210) and the Natural Science Foundation of Shandong Province (ZR2020MB018, ZR2022QE033 and ZR2021QB049).

Conflicts of interest

All authors declared that there are no conflicts of interest.

Ethical approval and consent to participate

Not applicable.

Consent for publication

Not applicable.

Copyright

© The Author(s) 2024.

REFERENCES

1. Foote, C. S. Mechanisms of photosensitized oxidation. There are several different types of photosensitized oxidation which may be important in biological systems. *Science* **1968**, *162*, 963-70. DOI PubMed
2. Chen, B.; Wu, L. Z.; Tung, C. H. Photocatalytic activation of less reactive bonds and their functionalization via hydrogen-evolution cross-couplings. *Acc. Chem. Res.* **2018**, *51*, 2512-23. DOI PubMed
3. Chen, R.; Wang, Y.; Ma, Y.; et al. Rational design of isostructural 2D porphyrin-based covalent organic frameworks for tunable photocatalytic hydrogen evolution. *Nat. Commun.* **2021**, *12*, 1354. DOI PubMed PMC
4. Meng, Q. Y.; Zhong, J. J.; Liu, Q.; et al. A cascade cross-coupling hydrogen evolution reaction by visible light catalysis. *J. Am. Chem. Soc.* **2013**, *135*, 19052-5. DOI PubMed
5. Baptista, M. S.; Cadet, J.; Di, M. P.; et al. Type I and type II photosensitized oxidation reactions: guidelines and mechanistic pathways. *Photochem. Photobiol.* **2017**, *93*, 912-9. DOI PubMed PMC
6. Baptista, M. S.; Cadet, J.; Greer, A.; Thomas, A. H. Photosensitization reactions of biomolecules: definition, targets and mechanisms. *Photochem. Photobiol.* **2021**, *97*, 1456-83. DOI PubMed
7. Chen, Y.; Lu, L.; Yu, D.; Zhu, C.; Xiao, W. Visible light-driven organic photochemical synthesis in China. *Sci. China. Chem.* **2019**, *62*, 24-57. DOI
8. Bonesi, S. M.; Manet, I.; Freccero, M.; Fagnoni, M.; Albini, A. Photosensitized oxidation of sulfides: discriminating between the singlet-oxygen mechanism and electron transfer involving superoxide anion or molecular oxygen. *Chemistry* **2006**, *12*, 4844-57. DOI PubMed
9. Chen, D.; Xu, Q.; Wang, W.; Shao, J.; Huang, W.; Dong, X. Type I photosensitizers revitalizing photodynamic oncotherapy. *Small* **2021**, *17*, e2006742. DOI PubMed
10. Greer, A. Christopher Foote's discovery of the role of singlet oxygen [$^1O_2$ ($^1\Delta_g$)] in photosensitized oxidation reactions. *Acc. Chem. Res.* **2006**, *39*, 797-804. DOI PubMed
11. Arnaut, L. G.; Pereira, M. M.; Dąbrowski, J. M.; et al. Photodynamic therapy efficacy enhanced by dynamics: the role of charge transfer and photostability in the selection of photosensitizers. *Chemistry* **2014**, *20*, 5346-57. DOI PubMed
12. Zhao, J.; Wu, W.; Sun, J.; Guo, S. Triplet photosensitizers: from molecular design to applications. *Chem. Soc. Rev.* **2013**, *42*, 5323-51. DOI PubMed
13. Zhao, J.; Xu, K.; Yang, W.; Wang, Z.; Zhong, F. The triplet excited state of bodipy: formation, modulation and application. *Chem. Soc. Rev.* **2015**, *44*, 8904-39. DOI PubMed
14. Glaser, F.; Kerzig, C.; Wenger, O. S. Multi-photon excitation in photoredox catalysis: concepts, applications, methods. *Angew. Chem. Int. Ed. Engl.* **2020**, *59*, 10266-84. DOI PubMed
15. Zhang, Y.; Doan, B. T.; Gasser, G. Metal-based photosensitizers as inducers of regulated cell death mechanisms. *Chem. Rev.* **2023**, *123*, 10135-55. DOI PubMed
16. Karges, J. Clinical development of metal complexes as photosensitizers for photodynamic therapy of cancer. *Angew. Chem. Int. Ed. Engl.* **2022**, *61*, e202112236. DOI PubMed
17. Nguyen, V. N.; Zhao, Z.; Tang, B. Z.; Yoon, J. Organic photosensitizers for antimicrobial phototherapy. *Chem. Soc. Rev.* **2022**, *51*, 3324-40. DOI PubMed
18. Michelin, C.; Hoffmann, N. Photosensitization and photocatalysis - perspectives in organic synthesis. *ACS. Catal.* **2018**, *8*, 12046-55. DOI
19. Wang, D.; Lee, M. M. S.; Shan, G.; et al. Highly efficient photosensitizers with far-red/near-infrared aggregation-induced emission for in vitro and in vivo cancer theranostics. *Adv. Mater.* **2018**, *30*, e1802105. DOI PubMed
20. Wang, D.; Su, H.; Kwok, R. T. K.; et al. Rational design of a water-soluble NIR AIEgen, and its application in ultrafast wash-free cellular imaging and photodynamic cancer cell ablation. *Chem. Sci.* **2018**, *9*, 3685-93. DOI PubMed PMC
21. Liu, K.; Liu, Y.; Yao, Y.; et al. Supramolecular photosensitizers with enhanced antibacterial efficiency. *Angew. Chem. Int. Ed. Engl.* **2013**, *52*, 8285-9. DOI PubMed

22. Shao, L.; Pan, Y.; Hua, B.; et al. Constructing adaptive photosensitizers via supramolecular modification based on pillararene host-guest interactions. *Angew. Chem. Int. Ed. Engl.* **2020**, *59*, 11779-83. DOI PubMed
23. Cai, X.; Liu, B. Aggregation-induced emission: recent advances in materials and biomedical applications. *Angew. Chem. Int. Ed. Engl.* **2020**, *59*, 9868-86. DOI PubMed
24. Cao, S.; Shao, J.; Wu, H.; et al. Photoactivated nanomotors via aggregation induced emission for enhanced phototherapy. *Nat. Commun.* **2021**, *12*, 2077. DOI PubMed PMC
25. Hu, F.; Xu, S.; Liu, B. Photosensitizers with aggregation-induced emission: materials and biomedical applications. *Adv. Mater.* **2018**, *30*, e1801350. DOI PubMed
26. Li, J.; Wang, J.; Li, H.; Song, N.; Wang, D.; Tang, B. Z. Supramolecular materials based on AIE luminogens (AIEgens): construction and applications. *Chem. Soc. Rev.* **2020**, *49*, 1144-72. DOI PubMed
27. Xu, S.; Duan, Y.; Liu, B. Precise molecular design for high-performance luminogens with aggregation-induced emission. *Adv. Mater.* **2020**, *32*, e1903530. DOI PubMed
28. Qian, W.; Zuo, M.; Sun, G.; et al. The construction of an AIE-based controllable singlet oxygen generation system directed by a supramolecular strategy. *Chem. Commun.* **2020**, *56*, 7301-4. DOI PubMed
29. Zuo, M.; Qian, W.; Hao, M.; Wang, K.; Hu, X.; Wang, L. An AIE singlet oxygen generation system based on supramolecular strategy. *Chinese. Chem. Lett.* **2021**, *32*, 1381-4. DOI
30. Hu, Y.; Yin, S.; Liu, W.; Li, Z.; Chen, Y.; Li, J. Rationally designed monoamine oxidase A-activatable AIE molecular photosensitizer for the specific imaging and cellular therapy of tumors. *Aggregate* **2023**, *4*, e256. DOI
31. Cui, L.; Yu, S.; Gao, W.; Zhang, X.; Deng, S.; Zhang, C. Y. Tetraphenylenthene-based conjugated microporous polymer for aggregation-induced electrochemiluminescence. *ACS. Appl. Mater. Interfaces.* **2020**, *12*, 7966-73. DOI
32. Li, Y.; Zhang, D.; Yu, Y.; et al. A cascade strategy boosting hydroxyl radical generation with aggregation-induced emission photosensitizers-albumin complex for photodynamic therapy. *ACS. Nano.* **2023**, *17*, 16993-7003. DOI PubMed
33. Lam, K. W. K.; Chau, J. H. C.; Yu, E. Y.; et al. An alkaline phosphatase-responsive aggregation-induced emission photosensitizer for selective imaging and photodynamic therapy of cancer cells. *ACS. Nano.* **2023**, *17*, 7145-56. DOI PubMed
34. Wang, J. L.; Xia, F. W.; Wang, Y.; et al. Molecular charge and antibacterial performance relationships of aggregation-induced emission photosensitizers. *ACS. Appl. Mater. Interfaces.* **2023**, *15*, 17433-43. DOI PubMed
35. Lee, M. M. S.; Yu, E. Y.; Yan, D.; et al. The role of structural hydrophobicity on cationic amphiphilic aggregation-induced emission photosensitizer-bacterial interaction and photodynamic efficiency. *ACS. Nano.* **2023**, *17*, 17004-20. DOI PubMed
36. Xing, L.; Wang, Y.; Li, X.; et al. A novel strategy to construct artificial light-harvesting system based on aggregation-induced emission surfactants for photocatalysis. *Adv. Opt. Mater.* **2023**, *11*, 2201710. DOI
37. Wang, Y.; Ma, C.; Li, X.; et al. A novel strategy of constructing an artificial light-harvesting system based on a supramolecular organic framework for photocatalysis. *J. Mater. Chem. A.* **2023**, *11*, 2627-33. DOI
38. Kim, C. T. T.; Nhien, P. Q.; Khang, T. M.; et al. Controllable FRET behaviors of supramolecular host-guest systems as ratiometric aluminum ion sensors manipulated by tetraphenylethylene-functionalized macrocyclic host donor and multistimuli-responsive fluorescein-based guest acceptor. *ACS. Appl. Mater. Interfaces.* **2021**, *13*, 20662-80. DOI PubMed
39. Wang, P.; Zhang, C.; Liu, H. W.; et al. Supramolecular assembly affording a ratiometric two-photon fluorescent nanoprobe for quantitative detection and bioimaging. *Chem. Sci.* **2017**, *8*, 8214-20. DOI PubMed PMC
40. Tang, B.; Xu, W.; Xu, J. F.; Zhang, X. Transforming a fluorochrome to an efficient photocatalyst for oxidative hydroxylation: a supramolecular dimerization strategy based on host-enhanced charge transfer. *Angew. Chem. Int. Ed. Engl.* **2021**, *60*, 9384-8. DOI PubMed
41. Li, X.; Cheng, D.; Niu, K.; et al. Construction of supramolecular dimer photosensitizers based on triphenylamine derivatives and cucurbit[8]uril for photocatalysis. *J. Mater. Chem. A.* **2023**, *11*, 24911-7. DOI
42. Zhao, N.; Li, M.; Yan, Y.; et al. A tetraphenylethene-substituted pyridinium salt with multiple functionalities: synthesis, stimuli-responsive emission, optical waveguide and specific mitochondrion imaging. *J. Mater. Chem. C.* **2013**, *1*, 4640-6. DOI
43. Li, X.; Gu, J.; Zhou, Z.; Liu, W.; Gao, J.; Wang, Q. Precise control for the aggregation and deaggregation with the aid of a tetraphenylethylene derivative: luminescence modulation and sensing performance. *Dyes. Pigments.* **2020**, *172*, 107844. DOI
44. Samanta, S. K.; Maiti, K.; Manna, S. K.; et al. An aggregation-induced emission (AIE)-active fluorescent chemodosimeter for selective sensing of hypochlorite in water and solid state: Endogenous detection of hypochlorite in live cells. *Dyes. Pigments.* **2021**, *196*, 109758. DOI
45. Wang, G. B.; Wang, Y. J.; Kan, J. L.; et al. Construction of covalent organic frameworks via a visible-light-activated photocatalytic multicomponent reaction. *J. Am. Chem. Soc.* **2023**, *145*, 4951-6. DOI PubMed
46. Jiang, M.; Wang, Y.; Liu, H.; Yu, S.; Niu, K.; Xing, L. Construction of a novel pyrene-based two-dimensional supramolecular organic framework and the selective regulation of reactive oxygen species for photocatalysis. *J. Mater. Chem. A.* **2024**, *12*, 4752-60. DOI
47. Murugesan, K.; Sagadevan, A.; Peng, L.; Savateev, O.; Rueping, M. Recyclable mesoporous graphitic carbon nitride catalysts for the sustainable photoredox catalyzed synthesis of carbonyl compounds. *ACS. Catal.* **2023**, *13*, 13414-22. DOI
48. Lian, P.; Wang, K.; Liu, H.; et al. Reacting molecular oxygen with butanone under visible light irradiation: a general aerobic oxidation of alkenes, sulfides, phosphines, and silanes. *Org. Lett.* **2023**, *25*, 7984-9. DOI PubMed
49. Li, X.; Wang, Y.; Wang, Y.; et al. Construction of supramolecular dimer based on benzothiazole derivative through host–guest interaction for photocatalysis. *Carbon. Neutral.* **2023**, *2*, 689-98. DOI